

Near-field ptychography using lateral and longitudinal shifts

A.-L. Robisch¹, K. Kröger¹, A. Rack², T. Salditt¹

¹Institut für Röntgenphysik, Georg-August-Universität Göttingen,
Friedrich-Hund-Platz 1, Göttingen, Germany

²European Synchrotron Radiation Facility, 38043 Grenoble Cedex, France

E-mail: arobisc@gwdg.de, tsaldit@gwdg.de

1. The Fresnel scaling theorem

In this work propagation of wave fields is computed using the Fresnel near-field propagator

$$D_{\Delta_{1,2}}[\psi_1] = \mathcal{F}^{-1} \left[\mathcal{F}[\psi_1] \cdot \exp \left\{ -\frac{i\Delta_{1,2}}{2k} \cdot (q_x^2 + q_y^2) \right\} \right], \quad (1)$$

where \mathcal{F} and \mathcal{F}^{-1} are the Fourier transform and the inverse Fourier transform; q_x, q_y are reciprocal coordinates; x, y are real space coordinates; $k = \frac{2\pi}{\lambda}$ is the wave number with wavelength λ , $\Delta_{1,2}$ is the distance between two points 1 and 2 along the optical axis; ψ_1 is an arbitrary wave field in plane 1. In case that ψ_1 represents a cone beam at distance $\Delta_{f,1}$ behind the focus, it can be written in paraxial approximation as

$$\psi_1^{\text{conebeam}} = \exp(ik\Delta_{f,1}) \exp \left[\frac{ik}{2\Delta_{f,1}} (x_1^2 + y_1^2) \right]. \quad (2)$$

To account for cone beam geometry, i.e. point source illumination of the object at distance $\Delta_{f,1}$ with respect to the focal plane, the usual variable transformation according to the Fresnel scaling theorem is used [1], resulting in the geometric magnification

$$M = \frac{\Delta_{f,1} + \Delta_{1,\text{det}}}{\Delta_{f,1}}, \quad (3)$$

and effective propagation distance

$$z_{\text{eff}} = \frac{\Delta_{1,\text{det}}}{M}, \quad (4)$$

where $\Delta_{1,\text{det}}$ is the distance from plane 1 to the detector. Up to this transformation, the two geometries (plane wave and cone beam) depicted in figure 1(a) are thus equivalent.

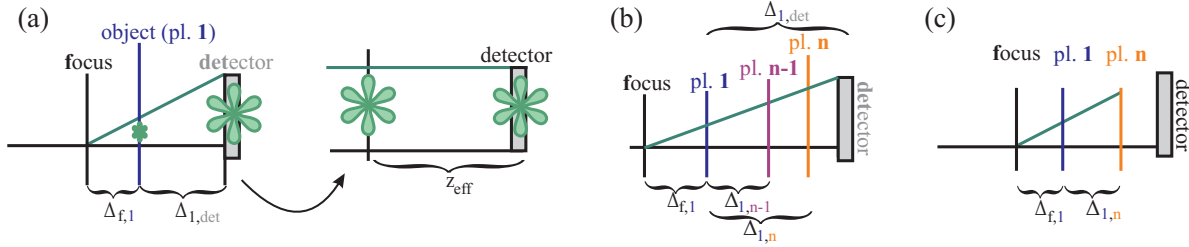


Figure 1. (a) The Fresnel scaling theorem allows to propagate a cone beam as a parallel beam, considering an effective geometry. (b) Effective geometry for propagating the exit wave. (c) Effective geometry for propagating the probe.

2. Cone beam propagation between multiple defocus planes

Generalizing ptychography with lateral and longitudinal shifts to cone beam geometry requires two different effective geometries: The propagation of the exit wave is performed using a coordinate system which is different from that used for the propagation of the probe between the different defocus planes. Figure 1(b-c) illustrates the effective propagation of (b) the exit wave, and (c) the probe. The magnification of the object $M_o^{(n)}$ depends on its distance relative to the focus

$$M_o^{(n)} = \frac{\Delta_{f,1} + \Delta_{1,\text{det}}}{\Delta_{f,1} + \Delta_{1,n}}. \quad (5)$$

Effective pixel sizes and effective propagation distances for the exit wave are

$$d_{\text{eff},o}^{(n)} = \frac{d}{M_o^{(n)}} \quad \text{and} \quad z_{\text{eff},o}^{(n)} = \frac{\Delta_{1,\text{det}} - \Delta_{1,n}}{M_o^{(n)}}. \quad (6)$$

Here d is the pixel size of the detector. For the propagation of the probe between defocus planes, the corresponding magnification $M_p^{(n)}$ according to figure 1(c) is

$$M_p^{(n)} = \frac{\Delta_{f,1} + \Delta_{1,n}}{\Delta_{f,1}}. \quad (7)$$

Effective pixel sizes and propagation distances are

$$d_{\text{eff},p}^{(n)} = \frac{d}{M_p^{(n)}} \quad \text{and} \quad z_{\text{eff},p}^{(n)} = \frac{\Delta_{1,n}}{M_p^{(n)}}. \quad (8)$$

Note that the product

$$M_p^{(n)} \cdot M_o^{(n)} = \max [M_o^{(n)}] = \text{const.} \quad (9)$$

This illustrates that a step wise effective propagation from one plane to the next and then to the detector results in the same magnification as a one-step propagation directly to the detector.

Two more statements can be made: First, the effective field of view (colored in green in figure 2) is the same for each defocus plane. As the detector is not moved closer to the focus, the information content in the gray shaded regions cannot be deduced from any measurements at detector distance $\Delta_{f,\text{det}}$ with respect to the focus. Second, since the effective pixel size of the probe $d_{\text{eff},p}^{(n)}$ decreases for defocus positions closer to the

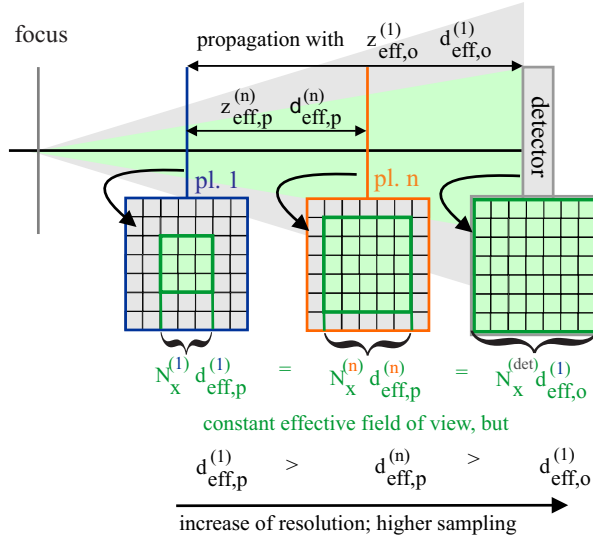


Figure 2. Effective propagation of the probe from plane 1 to plane n requires a larger pixel size and hence a coarser sampling than effective propagation from plane 1 to the detector. However the effective field of view (green) is constant for each plane. In order to avoid decreasing the resolution, a scaling factor $s^{(n)}$ is used to always propagate the probe with highest resolution $d_{\text{eff},o}^{(1)}$ while at the same time keeping the number of pixels and the effective field of view constant.

detector, the number of pixels, carrying information has to increase to keep the effective field of view constant (illustrated in the lower part of figure 2).

If effective propagation from plane 1 to plane n is to be performed, there are two possibilities: Starting from plane 1 with a complex valued field of highest resolution (as it resulted from an effective propagation of distance $z_{\text{eff},o}^{(1)}$ with pixel size $d_{\text{eff},o}^{(1)}$), one has to decrease the resolution to the pixel size $d_{\text{eff},p}^{(n)}$ before propagating to plane n . Once arrived at plane n and wanting to propagate to the detector, the resolution has to be increased again. This decreasing and increasing of resolution causes a loss of information and a lot of time for calculation.

The second and more efficient possibility is to keep the number of pixels with information content constant. For this reason the effective pixel size $d_{\text{eff},p}^{(n)}$ is scaled

$$\tilde{d}_{\text{eff},p}^{(n)} = d_{\text{eff},p}^{(n)} \cdot s^{(n)} \quad (10)$$

by the factor $s^{(n)}$

$$s^{(n)} = \frac{M_p^{(n)}}{\max [M_o^{(n)}]}, \quad (11)$$

which keeps the effective pixel size and hence the number of pixels carrying information constant for each defocus position.

3. An examination of near-field ptychography with respect to the twin image problem

As most phase retrieval algorithms are based on image propagation of the recorded intensities, the reconstructed object suffers from the well known twin image problem, see figure 3. Quantitative reconstructions therefore need additional constraints or additional diversity in the data, for example by recording multiple holograms. Here we investigate the suitability of lateral and longitudinal shifts to create this diversity, by further analysis

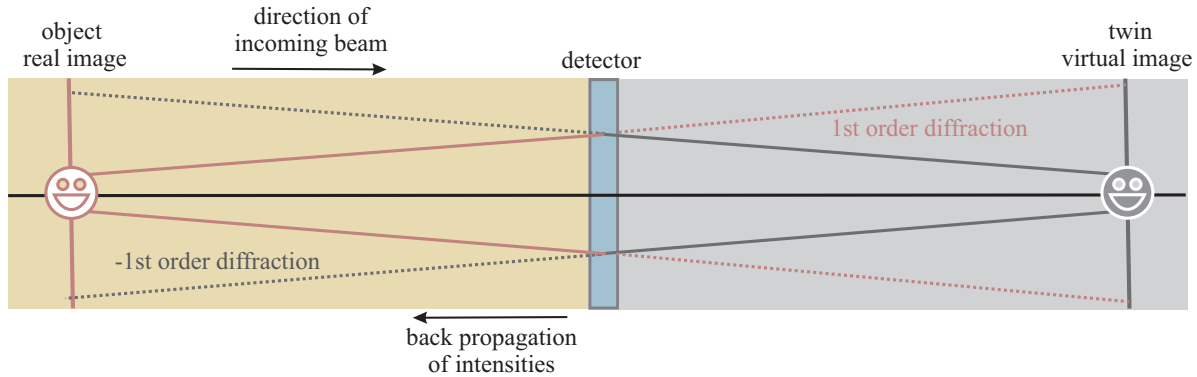


Figure 3. Illustration of the twin image problem. As it is well known, a hologram can be described by a superposition of the zeroth order diffraction, the first order diffraction and the minus first order diffraction, which results in the twin image (for example see [2, 3]). Numerical back propagation of the recorded intensities to the position of the object plane therefore results in the superposition of the sharp real image (first order, pink) and the out-of-focus contribution (minus first order, gray), while the opposite is true for the conjugate plane behind the detector.

of the data presented in the main manuscript. In particular, we show in figure 4 that both lateral and longitudinal shifts are required to remove twin image artifacts in object and probe.

To this end, we have taken the data as presented in figure 2(c) of the main manuscript, and have reconstructed it with either (figure 4(b)) only lateral shifts (compare to [4]) or (figure 4(c)) only longitudinal shifts, as compared to (figure 4(d)) the use of both, which was already shown in figure 1(c) of the main manuscript.

Only in the latter case, a satisfactory reconstruction of o and p can be achieved. Interestingly, case (b) yields a slightly better quality in the reconstruction of the probe aberrated by a beam modulating object than (c), while - even more clearly - the quality of the reconstructed object is better in (c) than in (b). However, none is as convincing as (d), which yields superior quality both for o and for p . Next, we propagate the reconstructed exit wave for each of the above cases (b, c, d) to two particular planes behind the detector (see sketch in figure 4(a)), namely the conjugated planes to the planes of the beam modulator and the object, i.e. the planes where the respective twin images would appear as sharp. Indeed, the twin images become visible for (b, c), while only defocused images are observed in (d), in line with the expectation for a high quality reconstruction without twin image artifacts. Note that the twin of the object is stronger in (b) than in (c). Only exploiting lateral diversity, a severely aberrated probe is needed for phase retrieval [4]. For nearly perfect probes, the collected (laterally shifted) holograms contain only redundant information and the reconstructions would show similar twin image features as a holographic reconstruction by back propagation. Contrarily, longitudinal shifts provide enough diversity for phase reconstruction of the object (overcoming the corresponding twin images), which has already been the base for many published multi-plane approaches [5, 6, 7], but fails with respect to probe

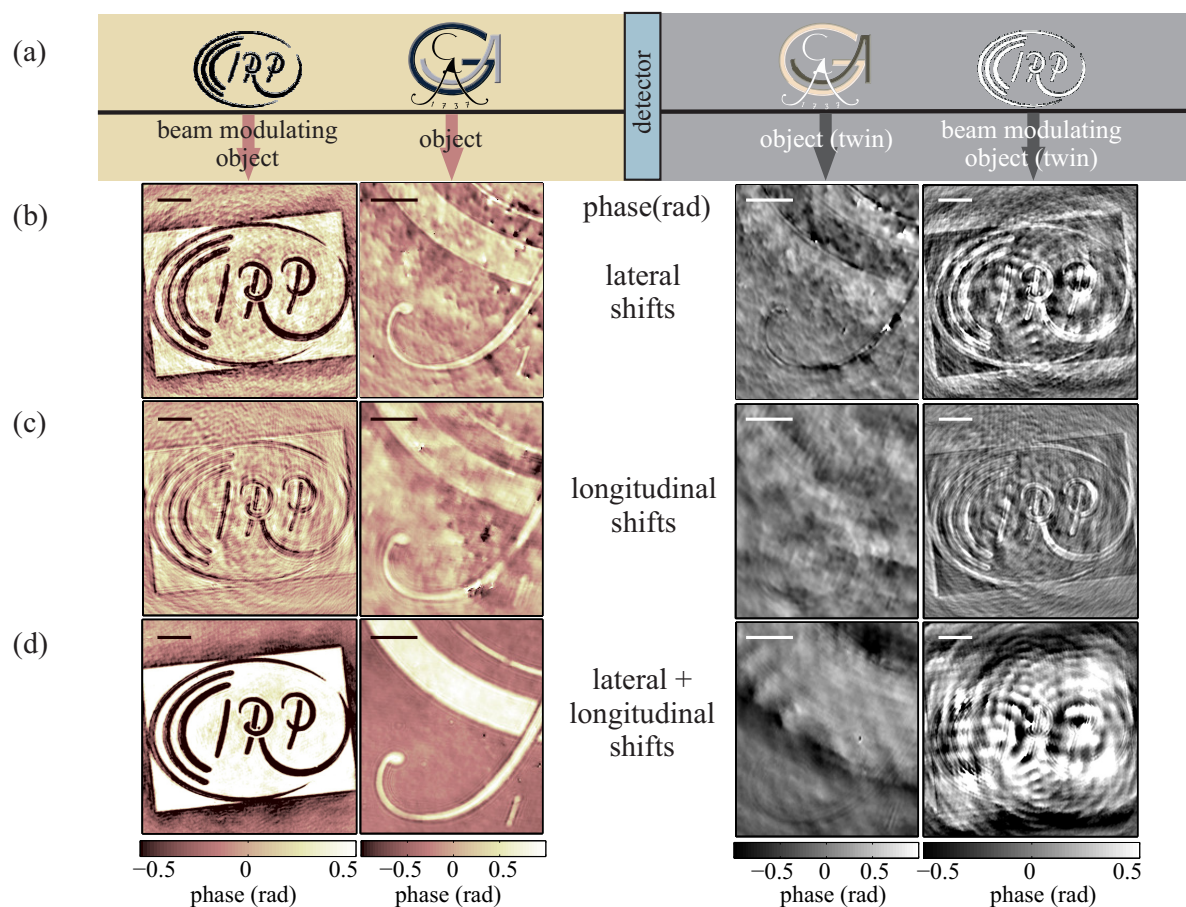


Figure 4. (a) Setup and location of the twin image planes with respect to the detector. (b) Reconstruction using holograms generated by only laterally shifting an object (left). Propagation of object and probe to their respective twin planes (right). (c) Reconstruction using holograms generated by only longitudinally shifting an object (left). Propagation of object and probe to their respective twin planes (right). (d) Reconstruction using holograms generated by laterally and longitudinally shifting an object (left). Propagation of object and probe to their respective twin planes (right). Scalebars denote 0.5 mm (probe) and 0.2 mm (object).

reconstruction. For this reason, additional empty beam recordings were necessary in [8], while the extended algorithm presented here is capable to reconstruct both o and p without any empty beam images, and without any further a priori information (support, weak object etc.).

References

- [1] Paganin D M 2006 *Coherent X-Ray Optics* (New York: Oxford University Press)
- [2] Onural L and Scott P D 1987 *Opt. Eng.* **26** 11241132
- [3] Yang S, Xie X, Zhao Y and Jia C 1999 *Opt. Commun.* **159** 29-31
- [4] Stockmar M, Cloetens P, Zanette I, Enders B, Dierolf M, Pfeiffer and Thibault P 2013 *Sci. Rep.* **3** 1927

- [5] Cloetens P, Ludwig W, Baruchel J, Van Dyck D, Van Landuyt J, Guigay J P and Schlenker M 1999 *Appl. Phys. Lett.* **75** 2912–4
- [6] Allen L J and Oxley M P 2001 *Opt. Commun.* **199** 65–75
- [7] Putkunz C T, Clark J N, Vine D J, Williams G J, Pfeifer M A, Balaur E, McNulty I, Nugent K A and Peele A G 2011, *Phys. Rev. Lett.* **106** 013903
- [8] Robisch A-L and Salditt T 2013 *Optics Express* **21** 23345–57